Geochemical Journal, Vol. 52, pp. e1 to e6, 2018 doi:10.2343/geochemj.2.0516

EXPRESS LETTER

Copper isotopic fractionation during adsorption on manganese oxide: Effects of pH and desorption

YUTA IJICHI,* TAKESHI OHNO and SHUHEI SAKATA

Department of Chemistry, Gakushuin University, Mejiro, Toshima-ku, Tokyo 171-8588, Japan

(*Received July 24, 2017; Accepted January 8, 2018; Online published March 5, 2018*)

We report new results for Cu^{2+} adsorption on δ-MnO_2 and the resulting changes in Cu isotopic composition due to isotopic fractionation. The adsorption experiments were designed as a pH series (3.22–6.94) and an adsorption-desorption series. ^{63}Cu adsorbs preferentially on δ-MnO_2, and the degree of isotopic fractionation is 0.45 ± 0.18‰ (2σ, n = 12). Preferential desorption of ^{65}Cu from δ-MnO_2 was also observed. The isotopic data are consistent with a closed isotopic equilibrium model, and the degree of fractionation indicates no systematic variation with pH or reaction time. Previously reported extended X-ray absorption fine structure study predicted the preferential adsorption of ^{65}Cu on δ-MnO_2, because of the formation of Cu^{2+} surface complexes (with 3–4 ligands) from dissolved Cu^{2+} (with 5 ligands); however, the opposite was observed in this study. The equilibrium in isotopic fractionation is affected by the bonding environment; hence, we suggest that dissolved Cu^{2+} species have a stronger bond than adsorbed ones.

Keywords: manganese oxide, adsorption, non-traditional isotope, Cu isotope fractionation, desorption

INTRODUCTION

Transition metal isotopic systems are commonly investigated to develop tracers for biogeochemical processes in the modern and ancient ocean. Ferromanganese oxide is an aggregate of iron and manganese oxyhydroxides, which scavenges many elements in the ocean. Recently, variations in isotopic composition of the adsorbed elements in natural ferromanganese oxides have been investigated to elucidate the paleo-redox conditions of ancient oceans and oceanic elemental circulation (Moynier *et al*., 2017). This requires an understanding of molecular-scale mechanisms of isotopic fractionation in naturally occurring elements. Interpretation of isotopic data from sedimentary records remains speculative for poorly understood mechanisms.

In the modern ocean, copper exists in a concentration of 0.5–6 nM (Takano *et al*., 2014). The vertical distribution of dissolved Cu^{2+} is affected by biological uptake and scavenging from settling particles (nutrient-scavenging hybrid types; Boyle *et al*., 1977). The speciation of dissolved Cu^{2+} in oceanic surface waters is dominated by complexation with organic ligands, resulting in low concentrations of free Cu^{2+} (Coale and Bruland, 1988).

Copper has two naturally occurring stable isotopes: ^{63}Cu (69.15% abundance) and ^{65}Cu (30.85%). Recent studies have shown that Cu^{2+} in deep marine waters has a heavier isotopic composition than in surface waters (Takano *et al*., 2014), with isotopically light Cu in surface waters being the result of mixing with river and rain waters. To achieve heavier Cu composition in deep waters, sedimentary sinks of ^{63}Cu, as ferromanganese oxides, are needed. It has been reported that isotopically light Cu^{2+} concentrations in natural ferromanganese nodules ($\delta^{65}Cu$ = 0.05–0.60‰; Albarède, 2004), crusts ($\delta^{65}Cu$ = 0.24–0.58‰; Little *et al*., 2014a) and modern seawater ($\delta^{65}Cu$ = 0.9–1.5‰; Vance *et al*., 2008) are comparable; this indicates preferential adsorption of ^{63}Cu on ferromanganese oxides.

In contrast, laboratory experiments have shown preferential adsorption of ^{65}Cu on Fe oxyhydroxides: $\Delta^{65}Cu_{soln\text{-}goethite}$ = –0.35 ± 0.11‰ (Clayton *et al*., 2005) and –0.8 ± 0.2‰ (Pokrovsky *et al*., 2008); and $\Delta^{65}Cu_{soln\text{-}ferrihydrite}$ = –0.78 ± 0.08‰ (Balistrieri *et al*., 2008). Extended X-ray absorption fine structure (EXAFS) studies have suggested that the heavier isotope is preferentially adsorbed onto manganese oxides because of the changes in the Cu^{2+} coordination environment (Sherman and Peacock, 2010; Little *et al*., 2014b).

Little *et al*. (2014b) suggested that the presence of dissolved organic Cu^{2+} complexes in the ocean could ex-

*Corresponding author (e-mail: 16142002@gakushuin.ac.jp)

plain inconsistencies between laboratory and oceanic experiments. Almost all the dissolved Cu^{2+} in seawater exists as organic complexes (>99%; Coale and Bruland, 1988). Heavier isotopes tend to favor a stronger bonding environment at chemical equilibrium (Bigeleisen and Mayer, 1947); therefore, ^{65}Cu tends to favor an association with dissolved organic ligands. Additionally, the Cu^{2+} isotopic composition of ferromanganese oxides is lighter than that of seawater because of the adsorption of residual ^{63}Cu (Little *et al*., 2014b). To elucidate the mechanisms of Cu^{2+} isotopic fractionation in nature, more laboratory experiments are needed, as in this study, where we investigated it during adsorption on δ-MnO_2. The direction of the isotopic fractionation related to adsorption of free Cu^{2+} ions on manganese oxides has been predicted (Sherman and Peacock, 2010); however, there is no experimental data concerning an isotopic fractionation factor. We discuss the mechanism of isotopic fractionation based on bond length and coordination using the predictions by EXAFS studies, and also emphasize the importance of the vibrational character of chemical bonds.

Experimental Method

Synthesis of oxides and preparation of Cu^{2+} solutions

The δ-MnO_2 was synthesized using a previously reported method (Foster *et al*., 2003) by simply mixing equal volumes of 30 mM $MnCl_2$ and 20 mM $KMnO_4$ solutions at pH 10 (adjusted by addition of KOH) in a polyethylene beaker. The suspensions were aged for 1 day and washed several times with ultrapure water. The precipitates were filtered using a 0.22-μm nitrocellulose filter, and freeze-dried. The crystalline oxides were identified by powder X-ray diffraction (XRD). The XRD pattern for δ-MnO_2 showed the characteristic peaks at 7.2, 3.6, 2.4, and 1.4 Å. δ-MnO_2 shows unclear peaks at 7.2 and 3.6 Å because of its low crystallinity. The crystalline fraction was monitored to ensure stability towards mineral transformations during storage. A δ-MnO_2 slurry, whose dry weight was determined before its use, was prepared without freeze-drying, for comparison with the freeze-dried δ-MnO_2.

The Cu^{2+} stock solution was prepared by dissolving $CuCl_2{\cdot}2H_2O$ (JIS Special Grade, Wako Pure Chemical Industries, Ltd., Japan) in ultrapure water, and the Cu^{2+} concentration was measured by inductively coupled plasma-mass spectrometry (ICP-MS: Agilent 7700; Agilent 8800).

Adsorption experiments

To avoid contamination of samples, all lab-wares were acid-washed and rinsed with ultrapure water (18.2 MΩ·cm, Milli-Q® Direct 8 System). HNO_3 (0.3 M) was used for washing, and the acid bath was continually monitored to check for contamination. HCl and HNO_3 used in experiments are high-purity chemical reagents (Ultrapure-100, Kanto Chemical, Japan).

Experiments were carried out to observe Cu^{2+} isotopic fractionation during its adsorption on δ-MnO_2, which was examined as a function of pH. The 20 mg of δ-MnO_2 used in each experiment were re-suspended in 10 mM KNO_3 solution, and then adjusted to an approximate target pH using NaOH or HNO_3. After at least 0.5 h of conditioning, an appropriate volume of the stock Cu^{2+} solution was added to achieve the required experimental Cu^{2+} concentrations. δ-MnO_2 has a low pH_{PZC} (2.25: Murray, 1974), thus the Cu^{2+} concentration in each experiment was set as higher than that in seawater ($[Cu^{2+}]$ = 1.57 mM in this study). 20-mL aliquots of mixed-metal suspension were placed in 50-mL polypropylene centrifuge tubes, and the pH-adjusted samples placed on an isothermal agitator (25°C, 170 rpm) overnight or for seven days.

The Cu^{2+} adsorption-desorption experiments were also conducted. The Cu^{2+} solutions were mixed with the δ-MnO_2 suspension. After one day, the suspension was filtered using a 0.22-μm nitrocellulose filter, and the solid phase was re-suspended in 20 mL of 10 mM KNO_3 solution. These suspension samples were then held for one more day to observe isotope effects during desorption. If the process was mainly controlled by an isotopic exchange equilibrium, equivalent isotope effects would be expected in both reaction directions (i.e., adsorption and desorption).

At the end of each experiment, the suspensions were filtered after pH measurement, and an aliquot was used for Cu^{2+} analysis to determine the fraction of Cu^{2+} adsorbed on the oxide. After filtration, we collected the solids remaining on the filter. Although the solid-phase samples were slightly wet, we did not rinse the solids on the filter to avoid desorption of Cu^{2+}. The residual solutions were evaporated to dryness and then re-dissolved in 10 M HCl; the solid phase samples were dissolved in 10 M HCl as well in order to prepare samples for anion-exchange chromatography.

Chemical separation

Anion-exchange chromatography was used to separate Cu^{2+} from the sample matrix (Maréchal *et al*., 1999). The columns (Muromac® polypropylene mini-columns, 7 × 60 mm) were loaded with 1 mL of BioRad® AG MP-1M anion-exchange resin. The resin was cleaned with 0.3 M HNO_3 and ultrapure water, then conditioned using 10 M HCl. The samples dissolved in 10 M HCl were loaded onto the columns, and most of the matrix and Mn^{4+} were eluted with 6 M HCl, before Cu^{2+} elution with 0.5 M HNO_3.

We regarded the degree of Cu^{2+} isotopic fractionation during chromatographic elution because it has already

Table 1. Summary of individual data from the adsorption experiment

Oxides	pH (final)	Adsorbed fraction of Cu	$\delta^{65}Cu_{soln}$ (‰)	$\delta^{65}Cu_{solid}$ (‰)	$\Delta^{65}Cu_{soln\text{-}solid}$ (‰)	Mass balance (‰)
δ-MnO_2	3.22	0.533 ± 0.016	0.23 ± 0.06	–0.28 ± 0.07	0.51 ± 0.09	–0.05 ± 0.05
	3.31	0.526 ± 0.011	0.27 ± 0.05	–0.33 ± 0.06	0.60 ± 0.08	–0.05 ± 0.04
	3.37	0.556 ± 0.010	0.21 ± 0.04	–0.27 ± 0.03	0.49 ± 0.05	–0.06 ± 0.03
	4.33	0.780 ± 0.011	0.36 ± 0.03	–0.07 ± 0.03	0.43 ± 0.05	0.02 ± 0.03
	5.10	0.950 ± 0.002	0.35 ± 0.06	0.04 ± 0.08	0.31 ± 0.11	0.06 ± 0.08
	6.94	0.999635 ± 0.000008	0.56 ± 0.13	–0.02 ± 0.04	0.58 ± 0.13	–0.02 ± 0.04
δ-MnO_2 (non-freeze-dried)	3.48	0.694 ± 0.018	0.21 ± 0.04	–0.16 ± 0.03	0.37 ± 0.05	–0.05 ± 0.03
	3.50	0.718 ± 0.008	0.20 ± 0.08	–0.13 ± 0.08	0.34 ± 0.11	–0.04 ± 0.06
	3.48	0.998190 ± 0.000016	0.45 ± 0.04	–0.01 ± 0.05	0.46 ± 0.06	–0.01 ± 0.05
δ-MnO_2 (7 days)	3.43	0.67 ± 0.02	0.20 ± 0.05	–0.31 ± 0.05	0.50 ± 0.08	–0.12 ± 0.06
	3.27	0.65 ± 0.03	0.23 ± 0.03	–0.24 ± 0.03	0.47 ± 0.05	–0.08 ± 0.03
	3.22	0.66 ± 0.03	0.21 ± 0.05	–0.20 ± 0.04	0.41 ± 0.06	–0.06 ± 0.03

The average delta value of Cu is n = 3 (40 plots per run).

been reported (Maréchal and Albarède, 2002). Therefore, the target element was fully recovered during elution. The eluate was evaporated to dryness to eliminate the HCl and the residue re-dissolved with 1 M HNO_3. Finally, Zn (for atomic absorption spectrometry: Kanto Chemical, Japan) was added as the external spike element after evaporation and re-dissolving in 0.3 M HNO_3.

Isotopic analysis

The isotopic composition of each experimental solution and solid phase was determined. All isotopic analyses were performed using multiple-collector ICP-MS (Nu Plasma). The mass bias derived from the instrument was corrected using a $^{68/66}Zn$ external correction based on an exponential law (Maréchal *et al*., 1999), as follows:

$$\left(\frac{^{65}Cu}{^{63}Cu}\right)_{corr} = \left(\frac{^{65}Cu}{^{63}Cu}\right)_{meas} \times \left[\left(\frac{^{68}Zn}{^{66}Zn}\right)_{ref} \Big/ \left(\frac{^{68}Zn}{^{66}Zn}\right)_{meas}\right]^{\ln\left(\frac{m65}{m63}\right)\Big/\left(\frac{m68}{m66}\right)} \quad (1)$$

where "corr" and "meas" represent the corrected and measured isotopic ratios, respectively, and "m" is the mass of the isotope. A standard-sample bracketing technique was employed to improve the reproducibility of the measurements. The isotopic data are expressed in δ notation relative to the initial Cu^{2+} solution, as follows:

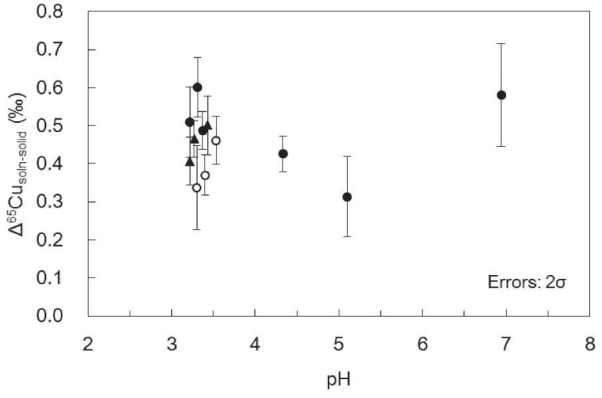

Fig. 1. $\Delta^{65}Cu_{soln\text{-}solid}$ (‰) versus pH in adsorption experiments with variable pH. ●: freeze-dried δ-MnO_2, ○: non-freeze-dried δ-MnO_2, ▲: freeze-dried δ-MnO_2 (7 days). Two sigma on this graph is an analytical error (n = 3).

$$\delta^{65}Cu(‰) = \left[\frac{\left(^{65}Cu/^{63}Cu\right)_{sample}}{\left(^{65}Cu/^{63}Cu\right)_{initialCu}} - 1\right] \times 1000. \quad (2)$$

RESULTS

Adsorption on δ-MnO_2

All adsorption experiments were conducted over 3 h, which was enough to attain a steady state. The adsorbed fraction in individual samples and the observed Cu^{2+} isotopic ratios are presented in Table 1. The fraction of adsorbed Cu^{2+} increased with increasing pH and Cu^{2+} was

Table 2. Summary of individual data from the adsorption-desorption experiment

Samples	pH (final)	Adsorbed fraction of Cu	$\delta^{65}Cu_{soln}$ (‰)	$\delta^{65}Cu_{solid}$ (‰)	$\Delta^{65}Cu_{soln\text{-}solid}$ (‰)	Mass balance (‰)
1-adsorption	3.28	0.7054 ± 0.003	0.224 ± 0.003		0.32 ± 0.04	0.05 ± 0.08
2-adsorption	3.23	0.7259 ± 0.016	0.34 ± 0.07		0.47 ± 0.10	0.026 ± 0.003
3-adsorption	3.25	0.7699 ± 0.010	0.333 ± 0.006		0.433 ± 0.009	0.026 ± 0.007
1-desorption	4.02	0.9703 ± 0.0006	0.39 ± 0.02	–0.04 ± 0.05	0.43 ± 0.05	
2-desorption	4.10	0.9670 ± 0.0018	0.35 ± 0.08	–0.110 ± 0.011	0.46 ± 0.08	
3-desorption	4.06	0.9659 ± 0.0013	0.34 ± 0.05	–0.081 ± 0.018	0.42 ± 0.05	

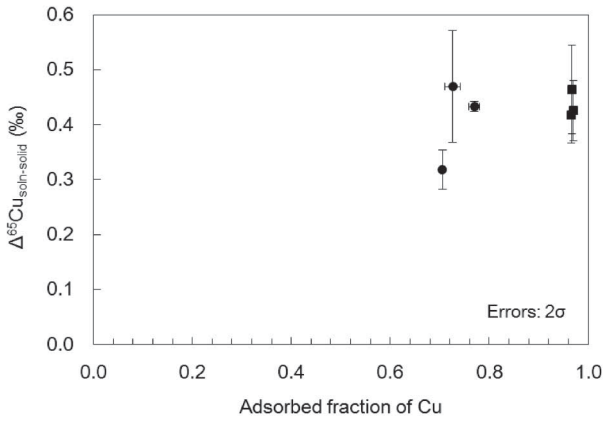

Fig. 2. Comparison of isotopic fractionation between Cu adsorption and desorption by δ-MnO_2 (●: adsorption, ■: desorption). Two sigma on this graph is an analytical error (n = 3). Heavy Cu isotope is concentrated in the liquid phase in both the adsorption and desorption reactions.

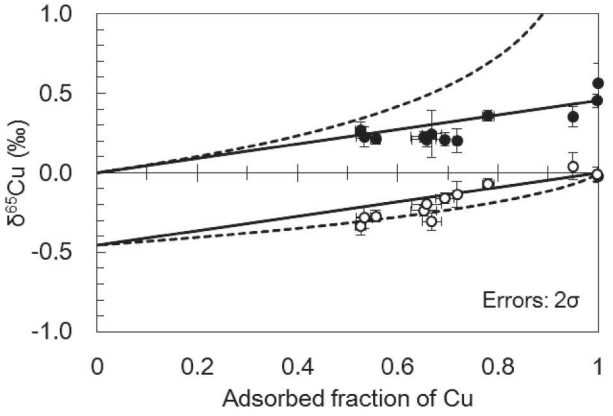

Fig. 3. $\delta^{65}Cu$ versus adsorbed fraction of Cu (●: $\delta^{65}Cu_{soln}$, ○: $\delta^{65}Cu_{solid}$). The parallel solid lines represent a closed isotope equilibrium model, and the curved dashed lines represent the Rayleigh fractionation model. All isotopic data from the solutions and solids from the adsorption experiments are plotted as a function of the fraction of Cu adsorbed to δ-MnO_2.

almost entirely adsorbed at pH ~ 8. The apparent largest adsorbed fraction, viz. that associated with the non-freeze-dried δ-MnO_2 at pH 3.48 (Table 1), was possibly caused by the low reproducibility concerning the amount of δ-MnO_2. About 0.33 mL of non-freeze-dried δ-MnO_2 was simply pipetted from bulk suspension; hence, we cannot know the actual weight of δ-MnO_2. ^{63}Cu preferentially adsorbed on δ-MnO_2 in a pH range of 3.3–6.9, and isotopic fractionation exhibited no systematic variation with pH (Fig. 1). The same isotopic fractionation also occurred in experiments with oxides that had been subjected to different storage methods or that had been conducted over a different duration time.

The degree of fractionation $\Delta^{65}Cu_{soln\text{-}solid}$ is defined as follows:

$$\Delta^{65}Cu_{soln\text{-}solid} = \delta^{65}Cu_{soln} - \delta^{65}Cu_{solid} \quad (3)$$

where $\delta^{65}Cu_{soln}$ and $\delta^{65}Cu_{solid}$ are the isotopic ratios of the experimental solution and solid, respectively. The average of all $\Delta^{65}Cu_{soln\text{-}solid}$ data is 0.45 ± 0.18‰ (2σ: experimental reproducibility, n = 12).

Table 2 and Fig. 2 show the results from the adsorption-desorption experiments. The magnitude of the isotopic fractionation associated with adsorption was calculated using the $\delta^{65}Cu_{soln}$ and the fraction of Cu^{2+} adsorbed on the solid (F); a batch model experiment (described in Subsection "Closed isotopic equilibrium model") was assumed because the solid phase was used for the desorption experiment. The isotopic fractionation related to the adsorption and desorption reactions were equivalents.

Discussion

Closed isotopic equilibrium model

The experimental data are consistent with a closed isotopic equilibrium model between dissolved and adsorbed Cu^{2+}. For a closed isotopic model, the relationship between the two phases can be described using isotopic mass balance, as follows:

$$\delta Me_{initial} = (\delta Me_{soln} \times [1 - F]) + (\delta Me_{solid} \times F) \quad (4)$$

where $\delta Me_{initial}$, δMe_{soln}, and δMe_{solid} are the initial, dissolved and adsorbed isotopic ratios of Cu^{2+}, respectively, and F is the fraction of Cu^{2+} adsorbed on the solid (δ-MnO_2). The applicability of a closed model can be explored by comparing isotopic data from experiments, using different adsorbed fractions and the experimentally determined fractionation factor, to the predictions for a closed-system and the Rayleigh fractionation model. The experimental data for $\delta^{65}Cu_{soln}$ and $\delta^{65}Cu_{solid}$ follow linear tends (Fig. 3), and are well matched with a closed-system model.

Mechanism of Cu^{2+} isotopic fractionation

The results indicate that the solution phase was enriched with ^{65}Cu during both the adsorption and desorption experiments, supporting the view that this fractionation process is controlled mainly by isotopic exchange equilibrium, rather than kinetic isotope effects. The degree of isotopic fractionation in chemical equilibrium usually depends on the reduced partition function ratio of the chemical species. This ratio is a function of temperature, relative mass difference, and vibrational frequency of the chemical bonds (e.g., Bigeleisen and Mayer, 1947). In our adsorption experiments, we considered that an isotope exchange reaction causes fractionation because of the difference between the reduced partition function ratio of dissolved and adsorbed species. Heavier isotopes tend to accumulate in stronger-bond environments (e.g., Bigeleisen and Mayer, 1947); therefore, it is suggested that dissolved Cu^{2+} has a stronger bond (a larger reduced partition function ratio) than that of adsorbed Cu^{2+}.

Comparison with EXAFS studies

Adsorption of Cu^{2+} on manganese oxides were studied by EXAFS because this technique could reveal the mechanisms of isotopic fractionation at the molecular scale (Manceau *et al*., 2002; Sherman and Peacock, 2010; Little *et al*., 2014b). The aqueous Cu^{2+} complex, assumed here to be the dissolved chemical species, has a distorted structure because of the Jahn-Teller effect. The aqueous Cu^{2+} complex has been represented as a six-coordinate complex, $Cu(H_2O)_6^{2+}$, with the two axial Cu-O bonds (2.38 Å) being longer than the four equatorial bonds (1.97 Å) (Fulton *et al*., 2000). The Cu^{2+} adsorbed on δ-MnO_2 is a six-coordinate complex as well (four equatorial (1.96 Å) and two axial (2.23 Å) Cu-O bonds; Manceau *et al*., 2002). Recently, however, a five-coordinate aqueous Cu^{2+} species was discovered, which has four equatorial (2.00 Å) and one axial (2.45 Å) Cu-O bonds (Amira *et al*., 2005). Moreover, three- or four-coordinate Cu^{2+} species were reported to adsorb on δ-MnO_2, as surface complexes over the vacancy sites of the oxides (Cu-O bond length = 1.95 Å: Sherman and Peacock, 2010). Under alkaline conditions (pH 8), some of the adsorbed Cu^{2+} become six-coordinate, with Cu-O bond lengths of 1.87–1.96 Å, by being incorporated into the oxide vacancies (Sherman and Peacock, 2010). The adsorbed Cu^{2+} species have shorter bonds than those of the dissolved species, regardless of pH. Thus, preferential adsorption of ^{65}Cu on δ-MnO_2 should occur because of the reduced bond lengths related to the change in the coordination environment.

The degree and direction of isotopic fractionation show no systematic variations according to the experimental data, even when the dominant Cu^{2+} species adsorbed on δ-MnO_2 changes from a surface complex to an incorporated species with increasing pH (Sherman and Peacock, 2010). Moreover, the observed direction of isotopic fractionation was opposite to that predicted by EXAFS studies (Sherman and Peacock, 2010; Little *et al*., 2014b). This most likely indicates differences in the vibrational character between the two phases, as well as in the bond lengths. There could be other factors controlling Cu^{2+} isotopic fractionation during adsorption on δ-MnO_2 rather than the coordination environment or bond length. More experimental isotopic data are needed to elucidate the mechanism of isotopic fractionation, with further laboratory and EXAFS studies.

Geochemical Implication

The degree and direction of Cu isotopic fractionation observed in this study are consistent with the ability of natural ferromanganese oxides to accumulate Cu^{2+} with lighter isotopic composition than that in seawater. Given that the Cu^{2+} in the ocean predominantly adsorbs on the MnO_2 phase in ferromanganese oxides (Little *et al*., 2014b), the isotopic composition of natural adsorbates should be controlled by the preferential adsorption of ^{63}Cu. Theoretical studies reported lighter isotopic compositions of the dissolved free Cu^{2+} than of its organic complexes, which are the dominant species in seawater. However, it is difficult to measure the isotopic fractionation between organic complexes and free Cu^{2+} ions. By estimating the isotopic fractionation during adsorption of free Cu^{2+} ions on manganese oxides, the fractionation between the organic complexes and free Cu^{2+} ions appears to be small. Hence, in addition to a theoretical estimative of isotopic fractionation, the nature of the organic ligands in seawater should be investigated.

Summary and Conclusions

1. In this study, we investigated the Cu^{2+} adsorption on δ-MnO_2. ^{63}Cu preferentially adsorbed on δ-MnO_2 and the degree of fractionation was given by $\Delta^{65}Cu_{soln\text{-}solid}$ =

0.45 ± 0.18‰ (2σ, n = 12).

2. The degree of isotopic fractionation during adsorption on δ-MnO_2 showed no systematic variation with pH or time under the experimental conditions (pH = 3.2–6.9; with duration of overnight to seven days). Isotopic exchange equilibrium reactions mainly control the fractionation.

3. In contrast, EXAFS studies predicted preferential adsorption of ^{65}Cu on δ-MnO_2 (Sherman and Peacock, 2010; Little *et al*., 2014b). However, there could be other factors controlling Cu^{2+} isotopic fractionation during adsorption on δ-MnO_2 rather than the coordination environment or bond length.

4. Investigation on the isotopic fractionation caused by chemical properties is useful and provides more direct data for predicting fractionation than EXAFS, which determines local structural information about the elements involved in isotopic fractionation.

5. ^{63}Cu preferentially adsorbs on δ-MnO_2 and its degree of isotopic fractionation is nearly equal to the difference in the Cu^{2+} isotope ratios between natural ferromanganese oxides and seawater. Hence, the effect of fractionation between Cu^{2+} organic complexes and free Cu^{2+} ions on the copper isotopic composition in deep sea might be small. It is necessary that future studies would identify these organic complexes and examine the relationship between the adsorbed Cu^{2+} species and the resulting isotopic fractionation.

Acknowledgments—We would like to thank M. Akaogi for the use of XRD. Financial support was provided to TO by Grants-in-Aid for Scientific Research from the Japan Society for Promotion of Science (Nos. 15H02149, 15H02630, 15K13586).

References

Albarède, F. (2004) The stable isotope geochemistry of copper and zinc. *Rev. Mineral. Geochem.* **55**, 409–427.

Amira, S., Spangberg, D. and Hermansson, K. (2005) Distorted five-fold coordination of Cu^{2+} (aq) from a Car-Parrinello molecular dynamics simulation. *Phys. Chem. Chem. Phys.* **7**, 2874–2880.

Balistrieri, L. S., Borrok, D. M., Wanty, R. B. and Ridley, W. I. (2008) Fractionation of Cu and Zn isotopes during adsorption onto amorphous Fe(III) oxyhydroxides: experimental mixing of acid rock drainage and ambient river water. *Geochim. Cosmochim. Acta* **72**, 311–328.

Bigeleisen, J. and Mayer, M. G. (1947) Calculation of equilibrium constants for isotopic exchange reactions. *J. Chem. Phys.* **15**, 261–267.

Boyle, E. A., Sclater, F. R. and Edmond, J. M. (1977) The distribution of dissolved copper in the Pacific. *Earth Planet. Sci. Lett.* **37**, 38–54.

Clayton, R. E., Hudson-Edwards, K. A. and Houghton, S. L. (2005) Isotopic effects during Cu adsorption onto goethite. *Geochim. Cosmochim. Acta* **69**, A216.

Coale, K. H. and Bruland, K. W. (1988) Copper complexation in the Northeast Pacific. *Limol. Oceanogr.* **33**, 1084–1101.

Foster, A. L., Brown, G. E., Jr. and Parks, G. A. (2003) X-ray absorption fine structure study of As(V) and Se(IV) sorption complexes on hydrous Mn oxides. *Geochim. Cosmochim. Acta* **67**, 1937–1953.

Fulton, J. L., Hoffmann, M. M., Darab, J. G., Palmer, B. J. and Stern, E. A. (2000) Copper (I) and copper (II) coordination structure under hydrothermal conditions at 325: an X-ray absorption fine structure and molecular dynamics study. *J. Phys. Hem. A* **104**, 11651–11663.

Little, S. H., Vance, D., Walker-Brown, C. and Landing, W. (2014a) The oceanic mass balance of copper and zinc isotopes, investigated by analysis of their inputs, and outputs to ferromanganese oxide sediments. *Geochim. Cosmochim. Acta* **125**, 673–693.

Little, S. H., Sherman, D. M., Vance, D. and Hein, J. R. (2014b) Molecular controls on Cu and Zn isotopic fractionation in Fe-Mn crusts. *Earth Planet. Sci. Lett.* **396**, 213–222.

Manceau, A., Lanson, B. and Drits, V. A. (2002) Structure of heavy metal sorbed birnessite. Part III: Results from powder and polarized extended X-ray absorption fine structure spectroscopy. *Geochim. Cosmochim. Acta* **66**, 2639–2663.

Maréchal, C. N. and Albarède, F. (2002) Ion-exchange fractionation of copper and zinc isotopes. *Geochim. Cosmochim. Acta* **66**, 1499–1509.

Maréchal, C. N., Telouk, P. and Albarède, F. (1999) Precise analysis of copper and zinc isotopic compositions by plasma-source mass spectrometry. *Chem. Geol.* **156**, 251–273.

Moynier, F., Vace, D., Fujii, T. and Savage, P. (2017) The isotope geochemistry of zinc and copper. *Rev. Mineral. Geochem.* **82**, 543–600.

Murray, J. W. (1974) The surface chemistry of hydrous manganese dioxide. *J. Coll. Interf. Sci.* **46**, 357–371.

Pokrovsky, O. S., Viers, J., Emnova, E. E., Kompantseva, E. I. and Freydier, R. (2008) Copper isotope fractionation during its interaction with soil and aquatic microorganisms and metal oxy(hydr)oxides: possible structural control. *Geochim. Cosmochim. Acta* **72**, 1742–1757.

Sherman, D. M. and Peacock, C. L. (2010) Surface complexation of Cu on birnessite (δ-MnO_2): controls on Cu in the deep ocean. *Geochim. Cosmochim. Acta* **74**, 6721–6730.

Takano, S., Tanimizu, M., Hirata, T. and Shorin, Y. (2014) Isotopic constrains on biogeochemical cycling of copper in the ocean. *Nat. Commun.* **5**, doi:10.1038/ncomms6663.

Vance, D., Archer, C., Bermin, J., Perkins, J., Statham, P. J., Lohan, M. C., Ellwood, M. J. and Mills, R. A. (2008) The copper isotope geochemistry of rivers and the oceans. *Earth Planet. Sci. Lett.* **274**, 204–213.